INSTITUTE OF PLASMA PHYSICS

NAGOYA UNIVERSITY

RESEARCH REPORT

NAGOYA, JAPAN

Dissipative Structure and Limit Cycle of Nonlinear Unstable Collisional Drift Mode

T. Hatori and Y. Terashima

IPPJ-250 June 1976

Further communication about this report is to be sent to the Research Information Center, Institute of Plasma Physics, Nagoya University, Nagoya 464, Japan.

Abstract

Based upon the model equations of quasilinear type, the nonlinear behaviour of the collisional drift instability is studied from a point of view of dissipative structure. It is shown that near marginal stability the drift mode is saturated to a nonlinearly stable state. As the ion viscosity decreases, bifurcation of nonlinear steady state occurs and no stable steady state is possible. The limit cycle appears instead of stationary solution. Particle transport is also estimated.

we here study the nonlinear development of the collisional drift instability, which occurs in the collisional regime of a magnetically confined plasma. Several works[1-3] have been done on this problem. Monticello and Simon[3] showed that the modification of the background density by the zero-frequency harmonic is the primary mechanism for saturation of the instability. Their treatment is mainly concerned with a steadily oscillating drift mode near marginal stability. We treat, from a point of view of dissipative structure[4], wider class of nonlinear problems such as the stability of nonlinear steady state itself and the transitions to higher instabilities besides saturation near marginal stability. Our asymptotic expansion scheme differs from those in the previous works[2,3]. We consider the conditions for electrostatic perturbation with the frequency ω and the wave numbers $k_\perp$, $k_\parallel$; $k_\perp^2 a_i^2 \ll 1$, $\Omega_e \gg \nu_{ei} \gg \omega$, $k_\parallel^2 D_{c\parallel}/\omega_* \gg 1$, where a_i is the mean ion gyroradius $a_i = v_{Ti}/\Omega_i$, Ω_α the cyclotron frequency of respective species, ν_{ei} the electron-ion collision frequency, ω_* the electron diamagnetic frequency and $D_{c\parallel}$ the classical diffusion coefficient along magnetic field, $D_{c\parallel} = 1.96\, T_e/m_e\nu_{ei}$ for the ions with unit charge. Under these conditions, the linear analysis[5] gives the frequency ω and the growth rate γ_L as

$$\omega = \omega_*/\{1+(1+\lambda)b\}, \quad \gamma_L = \omega_*(\omega_*-\omega)/k_\parallel^2 D_{c\parallel} , \tag{1}$$

where $\lambda = T_e/T_i$ and $b = \frac{1}{2} k_\perp^2 a_i^2$.

We start from the two fluid equations. After some procedure[3], we obtain the coupled equations for the density $n \simeq n_e \simeq n_i$ and the

electrostatic potential ϕ

$$\frac{\partial n}{\partial t} + \vec{u}_E\cdot\vec{\nabla}n + D_{c\parallel}\nabla_\parallel^2\left(\frac{e\phi}{T_e} - \log n\right) - \vec{\nabla}_\perp\cdot(D_{c\perp}\vec{\nabla}n) = Q_e \quad , \quad (2)$$

$$\frac{\partial n}{\partial t} + \vec{u}_E\cdot\vec{\nabla}n - \vec{\nabla}_\perp(D_{c\perp}\vec{\nabla}_\perp n) + \mathrm{div}\{\frac{n}{\Omega_i}\frac{\vec{B}}{B}\times[\frac{\partial}{\partial t} + (\vec{u}_E+\vec{u}_{di})\cdot\vec{\nabla}_\perp]\vec{u}_E\}$$

$$+\mathrm{div}\{\frac{n}{\Omega_i}\frac{\vec{B}}{B}\times[(\frac{\partial}{\partial t} + \vec{u}_E\cdot\vec{\nabla}_\perp)\vec{u}_{di} + \frac{1}{m_i}\vec{\nabla}_\perp \Pi_{FLR}(\vec{u}_\perp=\vec{u}_E)]\}$$

$$+ \mathrm{div}\{\frac{1}{m_i\Omega_i}\frac{\vec{B}}{B}\times\vec{\nabla}_\perp\Pi_s(\vec{u}_\perp=\vec{u}_E + \vec{u}_{di})\} = Q_i \quad , \quad (3)$$

where $T_{e,i}$ are supposed to be constants. $D_{c\perp}$ is the classical diffusion coefficient, $D_{c\perp}=(T_e+T_i)\,\nu_{ei}/m_e\Omega_e^2$, Π_s is the ion viscosity part of the stress tensor and Π_{FLR} is the finite ion gyroradius one, $\vec{u}_E=(c/B^2)\vec{B}\times\vec{\nabla}\phi$, and $\vec{u}_{di}=-(T_i/m_i\Omega_i)(\vec{B}\times\vec{\nabla}n)/Bn$. The sources $Q_{e,i}$ are introduced only to ascertain equilibrium.

We apply these equations to a slab model with the unperturbed density $N(x)=N_0(1+\kappa x)$ distributed in $0\le x\le \ell$ and the uniform magnetic field $\vec{B}=B\hat{z}$. The unperturbed potential is taken to be zero for brevity. We choose as a smallness parameter $\varepsilon\equiv|\kappa|\ell$ and intorduce the ordering scheme;

$$\omega/\Omega_i \sim \omega_*/\Omega_i \sim O(\varepsilon) \quad , \quad k_y\ell \sim O(1),$$

$$k_\parallel^2 D_{c\parallel}/\omega_* \sim O(1/\varepsilon),\ k_y^2 D_{c\perp}/\omega_* \sim O(\varepsilon) \text{ and } \nu_{ii}/\Omega_i \sim O(\varepsilon^2) \quad ,$$

$$\rho = \varepsilon\rho^{(1)} + \varepsilon^2\rho^{(2)} + \cdots\cdots, \quad \psi = \varepsilon\psi^{(1)} + \varepsilon^2\psi^{(2)} + \cdots \quad ,$$

$$\frac{\partial}{\partial t} = \varepsilon\frac{\partial}{\partial t_1} + \varepsilon^2(\frac{\partial}{\partial t_2} - v_g\frac{\partial}{\partial y_1}) + \cdots\cdots \quad ,$$

$$\frac{\partial}{\partial y} = \frac{\partial}{\partial y_0} + \varepsilon\frac{\partial}{\partial y_1} + \cdots \quad ,$$

where $\rho \equiv \tilde{n}/N(x)$ $(n=N+\tilde{n})$, $\psi \equiv e\tilde{\phi}/T_e$, and $\vec{v}_g$ is the group velocity to be determined in third order calculation. By this ordering, Eqs.(2) and (3) can be expanded in a systematic way[6]. Since calculation is rather lengthy, we will omit it here and quote only the results necessary for present arguments.

To the first order in ε, Eq.(2) is reduced to $D_{C_n}(n=N_0)\partial^2/\partial z^2 (\rho^{(1)}-\psi^{(1)})=0$, then we may write

$$\rho^{(1)} = \psi^{(1)} = h(x, t_2 \equiv \varepsilon^2 t) + \sum_{k_n, k_y} f(x, t_2) e^{i(k_y y_0 + k_n z - \omega t_1)} , \tag{4}$$

where h is the modulation of the background density, f the amplitude of the drift wave. Note that ω is taken to be real in this paper. In the second order ε^2, we find the dispersion relation for ω and the phase shift between $\rho^{(2)}$ and $\psi^{(2)}$ which is proportional to γ_L in Eq.(1). The nonlinear equations for h and f are obtained from the third order calculations, which after some simplifications are expressed in dimensionless form as

$$\frac{\partial H}{\partial \tau} = \left(\alpha \frac{\partial^2}{\partial \xi^2} - \eta \frac{\partial^4}{\partial \xi^4}\right) H + 2\frac{\partial}{\partial \xi}(F \Delta F), \tag{5}$$

$$\frac{\partial F}{\partial \tau} = \left(1 - \frac{\partial H}{\partial \xi}\right)(-\Delta F) - \eta \Delta^2 F, \tag{6}$$

where we set $H=(\pi/|\kappa|\ell)h$, $F=(\pi/|\kappa|\ell)f$, $\xi=\pi x/\ell$, $k=k_y\ell/\pi$, $\Delta=\partial^2/\partial\xi^2 - k^2$, $\tau=\gamma_L t/k^2$ and α is proportional to $D_{C\perp}$, $\alpha=k_y^2 D_{C\perp}/\gamma_L$ and η corresponds to viscosity damping, $\eta=(3/10)\nu_{ii}\lambda(k_y\pi/\ell)^2 a_i^4/4\gamma_L \equiv \eta_v/\gamma_L$.

These equations are of quasi-linear type, and will describe well the nonlinear behaviour of the drift wave. Without loss of generality, we hereafter may fix $k_{\parallel}$ and k_y values. In experiments, $k_{\parallel}$ is usually specified by the length of device or by the configuration of the magnetic field[7] and k_y takes a discrete value since the y direction corresponds to the θ direction of plasma column.

We now require the fixed boundary conditions at x=0, ℓ. Eqs.(5) and (6) can easily be solved by decomposing F and H into the Fourier components

$$F=\sum_p F_p \sin(p\xi) \quad \text{and} \quad H=\sum_p H_p \sin(p\xi). \tag{7}$$

The model eqs.(5) and (6) can be transformed into the form

$$\frac{d}{d\tau} H_p = -\Gamma_p H_p + \sum_{p',p''} K_{pp'p''} F_{p'} F_{p''} \quad , \tag{8}$$

$$\frac{d}{d\tau} F_p = \gamma_p F_p - \frac{1}{2} \sum_{p',p''} K_{p'pp''} H_{p'} F_{p''} \quad , \tag{9}$$

where $\Gamma_p=\alpha p^2+\eta p^4$ and $\gamma_p=\{1-\eta(p^2+k^2)\}(p^2+k^2)$ and with the Kronecker $\delta_{p,p'}$ $K_{pp'p''}=p(p''^2+k^2)(-\delta_{p,p'+p''}+\delta_{p,p''-p'}+\delta_{p,p'-p''})$

Based upon (8) and (9) we obtain the following results for successive transitions to higher instabilities

(1) The equilibrium: if $\eta>\eta_c\equiv 1/(1+k^2)$, there is no unstable mode, namely the steady state with $F_p=H_p=0$ is stable, which is indicated by the notation S[0].

(2) The first stage: if $\eta_c>\eta>\eta_1\equiv 1/(4+k^2)$, one mode F_1 become unstable associated with the back ground modulation H_2.

This stage is described by a simple set of the equations of two mode coupling,

$$\frac{d}{d\tau}H_2 = -\Gamma_2 H_2 - 2(1+k^2)F_1^2 \ , \tag{10}$$

$$\frac{d}{d\tau}F_1 = \gamma_1 F_1 + (1+k^2)H_2 F_1 \ . \tag{11}$$

Then we have the steady state, S[1], with the saturation levels,

$$F_{1S} = \pm\{(\eta_c - \eta)/\sqrt{2}\}^{1/2} \ , \ H_{2S} = \eta/\eta_c - 1 \ . \tag{12}$$

It is easy to confirm the nonlinear stability of this state. The state S[1] has a kind of dissipative structure[4]. In the moving frame with velocity $\vec{V}_* = \hat{y}T_e|\kappa|/m_e\Omega_e$, convective pattern for the ion fluid velocity is traced analogous to particle trapping in phase space, while the electrons show almost no convection. The saturation mechanism is mathematically made clear by the flow pattern as shown in Fig.1.

The enhanced diffusion coefficient is estimated from (12) to be

$$D_\perp = \{1 + [2 + \frac{3\sqrt{2}}{5}\frac{T_e}{T_e+T_i}(\frac{T_e}{T_i})^{3/2}(\frac{m_i}{m_e})^{1/2}(\frac{a_i\pi}{\ell})^2](1-\frac{\eta}{\eta_c})\}\, D_{c\perp}. \tag{13}$$

(3) The second stage: if $\eta_1 > \eta > 1/(9+k^2)$, two modes, F_1 and F_2, become unstable, associated with H_1 and H_2. We denote the new steady state with the finite amplitudes of $F_{1,2}$ and $H_{1,2}$ by S[2]. The steady state S[0] and S[1] remain to be the solutions in this stage. We find the bifurcation of the steady state.

It is interesting to see that all the S[0], S[1] and S[2] become unstable. Numerical computation shows that the trajectories of the solutions tend to a time-dependent asymptotic state, or in mathematical word limit-cycle around the S[1], as shown in Fig.2.

(4) In the case where $\eta<<1$: there exist many unstable modes. One cannot obtain the stationary profile of the background density and expects that the time-averaged asymptotic profile except in the boundary regions is a plateau, which is of course the solution of Eqs.(5) and (6). In both the ends of the slab, however, the steady "boundary layers" appear, of which the width is estimated to be $\ell\sqrt{\eta}$ by the critical wave number k_c making the growth rate γ_p vanish. In the plateau regime the drift waves carry most of the particle flux, but on the contrary in the boundary layers the classical transport is dominant over the wave transport. Therefore, the asymptotic value of the particle flux can be estimated to be the classical flux times $(\ell/2 - \ell\sqrt{\eta})/\ell\sqrt{\eta}$, the ratio of the density gradient in the boundary layer to the unperturbed value $N_0|\kappa|$. The effective diffusion coefficient is thus found to be of the order of

$$D_\perp \sim D_{c\perp}/2\sqrt{\eta} \ . \qquad (14)$$

References

1. T.H. Stix, Phys. Fluids 12, 627 (1969).

2. F.L. Hinton and C.W. Horton Jr., Phys. Fluids 14, 116 (1971).

3. D.H. Monticello and A. Simon, Phys. Fluids 17, 791 (1974).

4. P. Gransdorff and I. Prigogine, Thermodynamic Theory of Structure, Stability and Fluctuations, (Wiley-Interscience, 1971).

5. For example, A.A. Rukhadze and V.P. Silin, Usp.Fiz.Nauk 96, 87(1968) [Soviet Phys. Uspekhi, 11, 659 (1969)].

6. T. Hatori and Y. Terashima, submitted to J. Phys. Soc. Japan.

7. K. Kawahata and M. Fujiwara, J. Phys. Soc. Japan 14, 1150 (1976).

Figure Captions

Fig.1 The flow pattern of the dynamical system (10) and (11) is (c) the flow with two spiral attracters S[1] and one saddle point S[0] which is the superposition of (a) the cusp type flow corresponding the linear part and (b) the circulation type one with sinks and sorces representing the nonlinearity. The length of the arrows is proportional to the magnitude of the flow velocity.

Fig.2 Trajectories in (H_2, F_1) and (H_1, F_2) spaces of a numerical solution in the second stage. They start from points near the equilibrium S[0]. The trajectory (H_2, F_1) space first approaches S[1], goes away spirally and asymptotically forms a limit cycle around S[1]. In (H_1, F_2) space, the trajectory grows monotonously to a limit cycle. The period of the cycle in (H_1, F_2) space is twice the one in (H_2, F_1).

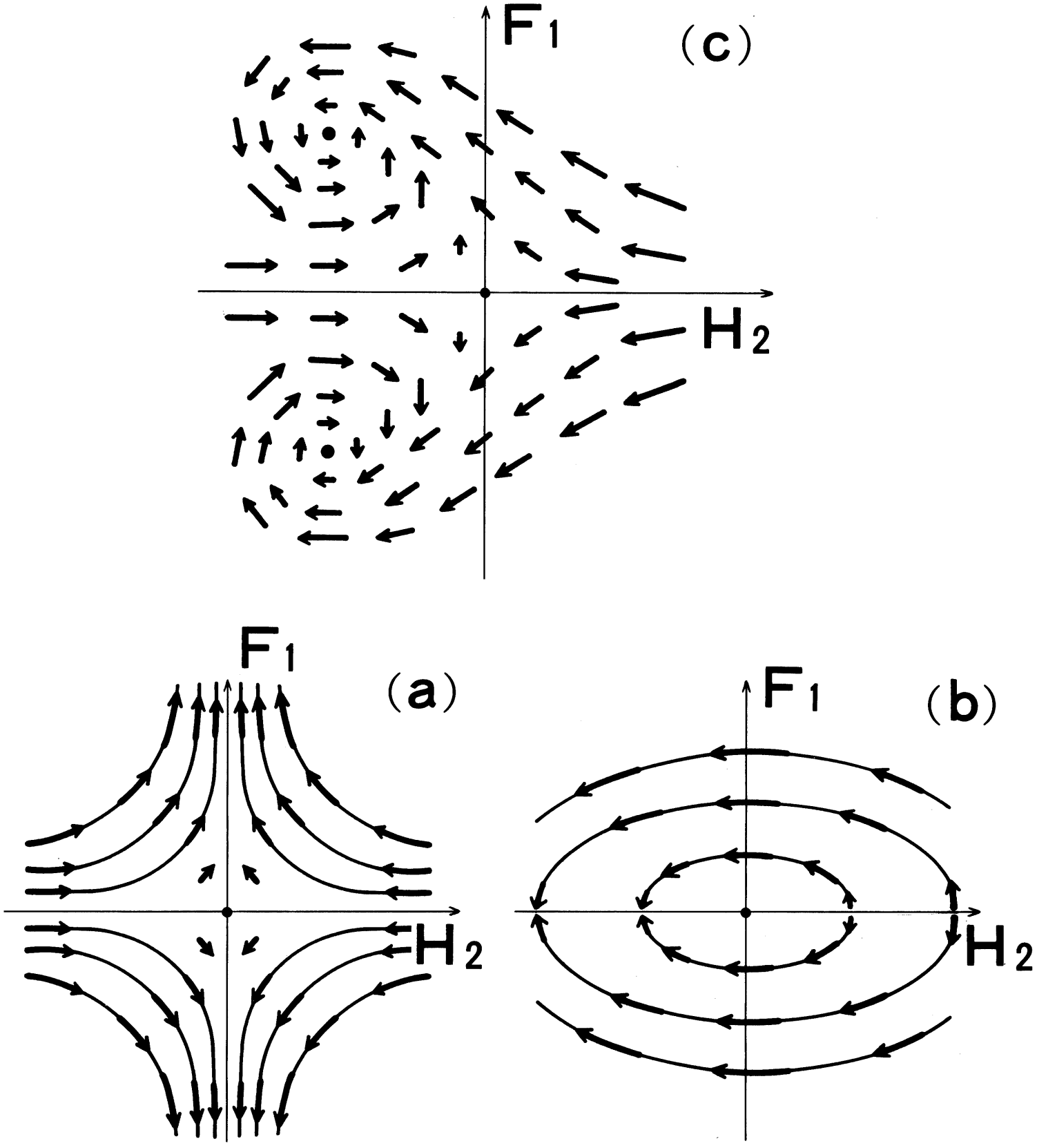

FIG. 1

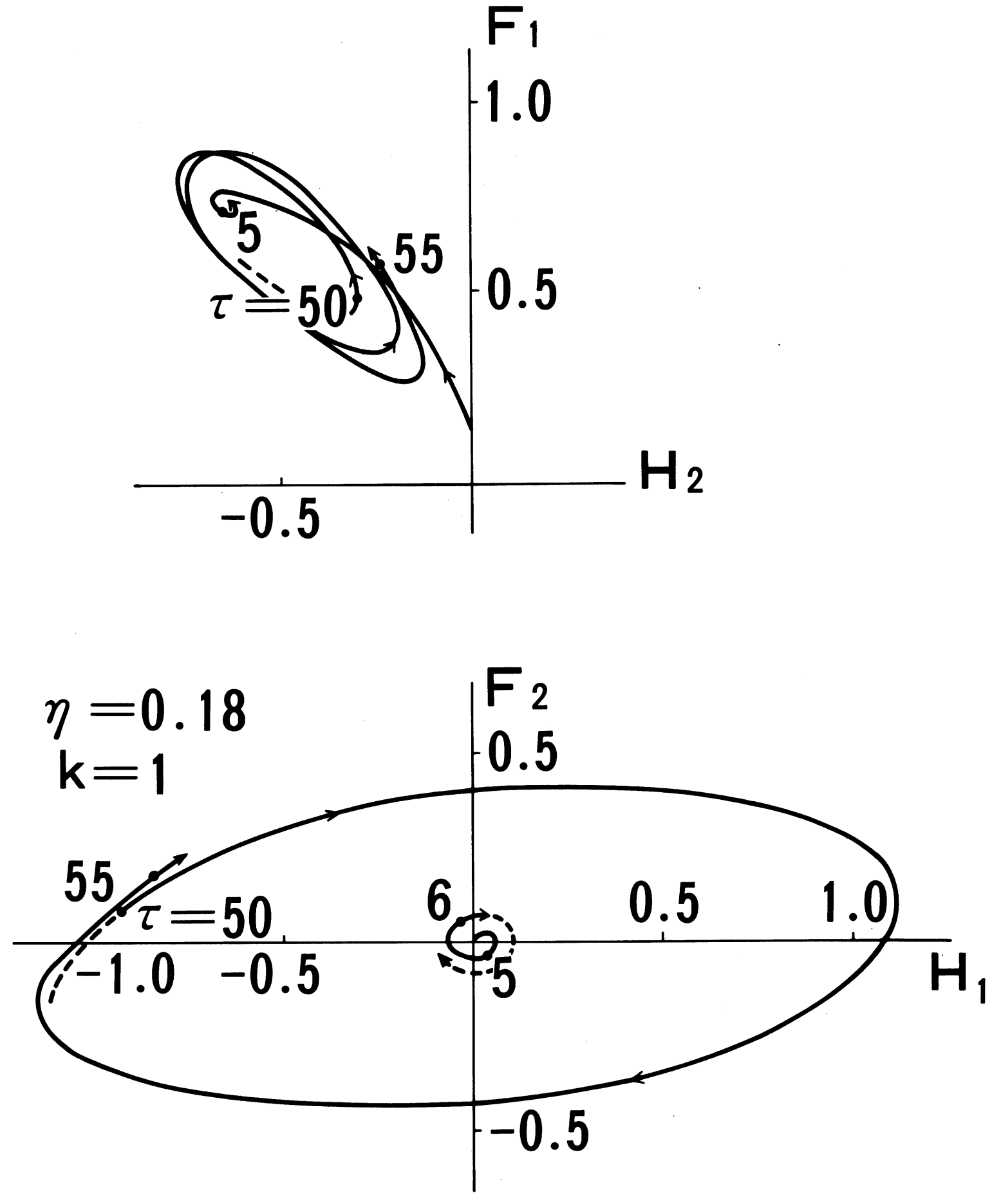

FIG. 2